macromol

MDPI

Article

Polyvinyl Alcohol Films Reinforced with Nanocellulose from Rice Husk

Gabriel Monteiro Cholant [1], Mariane Weirich Bosenbecker [1], Alexandra Augusta Reichert [1], Cesar Augusto Gonçalves Beatrice [2], Thales Castilhos Freitas [3], Naurienni Dutra Freitas [1], Nathalia Vieira Villar de Nunes [1], Alexandre Ferreira Galio [4], André Luiz Missio [1,*] and Amanda Dantas de Oliveira [1]

[1] Technological Development Center—CDTec, Postgraduate Program in Materials Science and Engineering—PPGCEM, Federal University of Pelotas—UFPel, Pelotas 96010-610, RS, Brazil; gabriel.scholant@homail.com (G.M.C.); marianbosenbecker@hotmail.com (M.W.B.); alereichert94@yahoo.com.br (A.A.R.); naurienni@gmail.com (N.D.F.); nathaliannunes@gmail.com (N.V.V.d.N.); adoliveira@ufpel.edu.br (A.D.d.O.)

[2] Department of Materials Engineering, Federal University of São Carlos—UFSCar, São Carlos 13565-905, SP, Brazil; cagbeatrice@gmail.com

[3] Graduate Program in Biodiversity and Nature Conservation (PPGBiodiversidade), Federal University of Juiz de Fora—UFJF, Juiz de Fora 36036-900, MG, Brazil; thales.castilhos@gmail.com

[4] Postgraduate Program in Materials Science and Engineering (PPCEM), Federal University of Pampa—UNIPAMPA, Bagé 96413-170, RS, Brazil; alexandregalio@unipampa.edu.br

* Correspondence: andre.missio@ufpel.edu.br

Abstract: Progress in the field of biodegradable materials has been significantly accelerated in recent years, driven by the search for sustainable substitutes for fossil-derived resources. This study investigates the formulation of biodegradable films composed of polyvinyl alcohol (PVA) and nanocellulose extracted from rice husk. The rice husk underwent alkaline treatment and bleaching for cellulose extraction, followed by sulfuric acid hydrolysis to obtain nanocellulose. The cellulose and nanocellulose were characterized through Fourier Transform Infrared Spectroscopy (FTIR), X-ray Diffraction (XRD), and Thermogravimetric Analysis (TGA). Films of pure PVA and those reinforced with 1 wt. % of nanocellulose were prepared using the solvent casting method. The evaluations showed that the modulus of elasticity and tensile strength of the PVA/nanocellulose films were increased by 295.45% and 29.6%, respectively, compared to the pure PVA film. The PVA/nanocellulose film exhibited the lowest solubility and water vapor permeability. Optical Microscopy confirmed a flawless surface for the nanocellulose-reinforced film, while the cellulose- and rice husk-reinforced films displayed irregularities. In the biodegradability assessment, the nanocellulose-reinforced film was the only one that withstood the experimental conditions. The results highlight the effectiveness of nanocellulose in enhancing PVA properties, making these films promising for sustainable packaging applications.

Keywords: agroindustrial waste; sustainable materials; composites; biodegradable; packaging

Academic Editor: Ana María Díez-Pascual

Received: 24 November 2024
Revised: 10 January 2025
Accepted: 29 January 2025
Published: 5 February 2025

Citation: Cholant, G.M.; Bosenbecker, M.W.; Reichert, A.A.; Beatrice, C.A.G.; Freitas, T.C.; Freitas, N.D.; de Nunes, N.V.V.; Galio, A.F.; Missio, A.L.; de Oliveira, A.D. Polyvinyl Alcohol Films Reinforced with Nanocellulose from Rice Husk. *Macromol* **2025**, *5*, 6. https://doi.org/10.3390/macromol5010006

1. Introduction

Recently, there has been a surge in research focused on biodegradable materials for packaging applications to reduce the impact on the environment caused by the exacerbated growth of petroleum-based synthetic polymers. Thus, biodegradable materials emerge as an alternative for the development of packaging and can replace synthetic polymers,

either as reinforcements or in blends. In this context, the use of raw materials from natural sources is gaining prominence due to their non-toxic nature, renewability, and abundance. This is exemplified by materials like cellulose, starch, chitosan, chitin, and others [1].

Recent studies have shown that reinforcing PVA with materials such as starch, chitosan, and bacterial cellulose can enhance mechanical and barrier properties [2–4]. Our study highlights the unique advantages of using rice husk-derived nanocellulose compared to these materials.

In this sense, the use of cellulose for the manufacture of biodegradable materials is related to the fact that this material is a natural polymer with a semi-crystalline structure and is present in an abundant form in the environment, and besides endowing the final product with a low cost, can increase the strength of the material. Its extraction can be performed by different methods, such as those using agricultural waste, wood, and bacteria. However, cellulose presents some limitations when incorporated into a polymeric matrix, such as affinity with some materials, and disadvantages regarding barrier properties, thus impairing the final material [5].

Therefore, nanocellulose serves as an alternative reinforcement for the development of biodegradable packaging. Generally, when added to a polymer matrix, it leads to an increase in the mechanical properties of the material compared to the pure polymer; this increase in the mechanical characteristics of the material is due to its large surface area, facilitating effective dispersion within the matrix. Furthermore, when used as reinforcement, nanocellulose enhances the material's barrier properties through its capacity to form hydrogen bonds, thus inhibiting the penetration of water molecules. Therefore, its use in the packaging industry is very promising in relation to adding important characteristics to the final material, besides providing a low cost and reducing the environmental impacts caused by synthetic polymers [6].

The production of agroindustrial byproducts encompasses a diverse spectrum, and relates to varied sectors engaged in the processing of agricultural derivatives. Nevertheless, the indiscriminate disposal of such residues has been instigating a succession of environmental predicaments, leading to the contamination of terrestrial and aquatic ecosystems through leaching phenomena [7]. Rice husk, a byproduct of agricultural activities, is notably rich in cellulose, constituting up to 38% of its composition. In terms of global production, rice contributes around 741 million tons, subsequently resulting in substantial quantities of rice husks due to the intricacies of the processing methodology [8].

Rio Grande do Sul is the largest rice producer in Brazil, accounting for approximately 70% of the country's rice production. Consequently, significant amounts of rice husks are generated as a byproduct of rice processing. However, the slow natural degradation of rice husks can lead to environmental issues, such as air and water pollution, if not properly managed. Therefore, valorizing this abundant agricultural waste by converting it into nanocellulose for polymer reinforcement presents an environmentally sustainable solution [9,10].

Thus, the use of biomass-based materials, such as rice husks, not only supports sustainable development, but also reduces carbon footprints, aligning with global sustainability goals [7,11].

Polyvinyl alcohol (PVA) is known for being a biodegradable polymer and non-toxic, and for its ability to form films, besides being biocompatible with natural fibers and presenting good optical transparency. The combination of PVA with natural fibers yields a material with excellent mechanical properties and a decrease in the cost of the final product when compared to the pure polymer, besides improving the barrier properties of the material. These characteristics impart the PVA with great potential for application as a matrix in biodegradable films [12].

Therefore, because of the above considerations, the present study aimed to use rice husk to obtain cellulose via alkaline treatment and bleaching, followed by isolating the nanocellulose through the process of acid hydrolysis. The intention was to add the reinforcement into a matrix of polyvinyl alcohol to develop biodegradable films via the solvent casting method, aiming at applying this material in packaging with improved properties and lower negative impacts, such as those generated by synthetic polymers.

This study stands out by demonstrating the potential of nanocellulose derived from rice husks to significantly improve the properties of PVA films, offering a sustainable and efficient alternative for biodegradable packaging. By focusing on rice husks generated in Rio Grande do Sul, the largest rice-producing region in Brazil, this research addresses a significant waste management challenge faced by the country's agricultural sector. The study promotes the sustainable use of agro-industrial residues, contributing not only to Brazil's efforts to develop eco-friendly materials, but also aligning with global commitments to sustainability, waste reduction, and the advancement of circular economies.

2. Materials and Methods

2.1. Materials

2.1.1. Rice Husk (RH)

The rice husk (RH) used in this study was donated by Cerealista Polisul, located in the city of Pelotas/RS. The husk was used as a fine powder and has been characterized during the development of this research.

2.1.2. Polyvinyl Alcohol (PVA)

The polymer utilized in this study was procured from Vetec, possessing a molar mass of 86.09 g/mol and an 87.84% hydrolysis index.

2.2. Extraction of Cellulose from Rice Husk

For CNC extraction, commercial brands of sodium hypochlorite (NaClO, Girando Sol), sodium hydroxide (NaOH), and sulfuric acid (H_2SO_4), acquired from Dinâmica Química Contemporânea LTDA in Brazil, were utilized. All solvents and reagents were applied without any further purification.

The procedure to the extraction of cellulose from rice husk was conducted following the methodology outlined by Bosenbecker et al. [13], with some adaptations. The extraction of cellulose from rice husk was performed in three steps: a pre-treatment of the husk in natural form, followed by the alkaline treatment, and finally, the bleaching. The husks were washed in running water and dried in an oven for 24 h at 50 °C to remove the humidity. After complete drying, the material was ground in a Marconi MA 340 knife mill and sieved with a 32 mesh sieve to maintain particle size uniformity.

After the process involving alkaline treatment, bleaching was performed, where the fiber was added in a solution of 2.5% w/v (fiber to sodium hypoclhorite) of sodium hypochlorite for 24 h in order to remove remaining components of lignin, thus obtaining the white color characteristic of cellulose. The resulting material was filtered and washed with distilled water until it reached neutral pH, then dried in an oven at 60 °C for 24 h [14]. Figure 1 illustrates the resulting material after the treatments involved.

Subsequently, the rice husk in natural form was submitted to alkaline treatment with a sodium hydroxide solution with a concentration of 10% w/v (10% NaOH in relation to the weight of the biomass), aiming to remove components of lignin and hemicellulose in the fiber. This concentration was determined through previous studies by the research group [14]. The fibers were in contact with this solution for 1 h at 80 °C under magnetic stirring. Following this, the fibers were separated through filtration and washed repeatedly

with distilled water until the filtration residue reached a neutral pH level. After pH adjustment, the fibers were dried in an oven at 50 °C for 24 h [15–17].

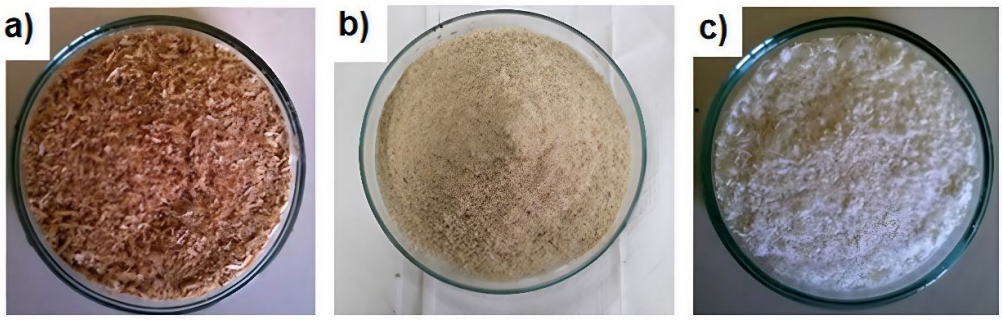

Figure 1. Images of: (**a**) rice husk in natura, (**b**) rice husk after pre-treatment, (**c**) pulp after alkaline treatment and bleaching.

2.3. Obtaining the Nanocellulose

The procedure to isolate nanocellulose (NC) from cellulose was conducted following the methodology outlined by Rashid and Dutta [5], with some adaptations. The process involved the acid hydrolysis of cellulose using 65% sulfuric acid at a ratio of 1:20 w/v (cellulose to sulfuric acid) for a duration of 90 min at 45 °C under ultrasound. The reaction was terminated by the addition of distilled water and centrifugation was performed in an Excelsa Centrifuge, model 206 BL, at 2260× RCF g or 12,000 rpm for 10 min to remove excess acid.

This centrifugation process was repeated five times until the supernatant was completely separated from the precipitate. Subsequently, the suspension was dialyzed using a 26 (Spectra/Por 6, MWCO = 3500 g/mol) dialysis membrane until it reached a neutral pH. Following dialysis, the suspension was freeze-dried in a freeze-dryer model MSSL-404 for 48 h under a pressure of 60 mm Hg and a temperature of −42 °C to obtain the nanocellulose in powdered form for material characterization.

2.4. Film Preparation

The solvent casting technique was used to prepare the PVA films with the respective rice husk, cellulose and nanocellulose reinforcements. The films were prepared with a fixed concentration of 1 wt. % by mass for each formulation; a control film of pure PVA was also prepared. The methodology adopted was from Kord et al. [18] with some modifications.

2.5. Characterization

2.5.1. Characterization of Rice Husk, Cellulose and Nanocellulose

Initially, a solution was concocted by combining 5 g of PVA and 1 g of glycerol in 95 mL of distilled water, subjected to a temperature of 70 °C for 60 min, under magnetic stirring to ensure the dissolution of PVA. Following this, the rice husk, cellulose, and nanocellulose reinforcements were integrated into the solution, maintaining constant stirring and a temperature of 45 °C to facilitate the uniform dispersion of the reinforcements within the matrix. The resultant solution, encompassing the reinforcements along with the control solution of unadulterated PVA, were each placed in 20 mL quantities onto glass plates (100 mm diameter) and subjected to a drying process within an oven for 24 h at a temperature of 40 °C to imitate water evaporation. Following the drying phase, the films were demolded and preserved for subsequent analyses [19].

$$IC = \frac{\mathrm{I}(002) - \mathrm{I}(\mathrm{am})}{\mathrm{I}(002)} \times 100 \quad (1)$$

where Iam is the intensity referring to the region of 2θ = 16°; I002 is the maximum intensity of the diffraction peak, attributed to the crystalline material, in the region of 2θ = 22°.

2.5.2. Film Characterization

Thickness, Weight and Density

To ascertain the thickness of the films, an external micrometer, spanning a range of 0 to 25 mm and boasting a reading precision of 0.01, manufactured by Eda Professional, was deployed. Measurements were executed at five disparate points for each film composition.

The thickness of the films was measured using a micrometer with a precision of 0.01 mm, at five different points for each sample. The pure PVA film showed an average thickness of 0.158 mm, with a standard deviation of ±0.050 mm, indicating moderate variation in thickness uniformity. The PVA film reinforced with rice husk exhibited an average thickness of 0.180 mm, with a standard deviation of ±0.029 mm, reflecting greater regularity. For the film reinforced with cellulose, the average thickness was 0.156 mm, with a standard deviation of ±0.040 mm. Finally, the PVA film with nanocellulose presented an average thickness of 0.222 mm, with a standard deviation of ±0.049 mm.

For the quantification of the film's weight, Equation (2) was employed [20]:

$$G = \frac{m}{A} \quad (2)$$

where the weight is represented by G (g/cm^2), the mass by m (g) and the area by A with a unit (cm^2). The films were cut with the same area of 16 cm^2 and weighed on an analytical balance [21]. The densities of the films were ascertained from the weight and dimensions of the films using Equation (3) [22]:

$$D = \frac{m}{A \times T} \quad (3)$$

where m is the mass (g), A is the area (cm^2), and T is the thickness of the films in(cm).

Transparency

The visual integrity and flexibility of the films were evaluated utilizing a camera with a resolution of 12 megapixels. A uniform distance of 10 cm was maintained for capturing transparency photographs across all film specimens [23].

Solubility

The solubility of the films was determined in adherence to the methodology delineated in Luchese et al. [24]. Three specimens, each dimensioned at 4 cm × 4 cm, were configured for each formulation. Initially, these specimens were oven-dried at 60 °C for a duration of 24 h to establish their inaugural weight. Subsequently, the films were submerged in a beaker containing 50 mL of distilled water at ambient temperature and agitated for a period of 24 h. Following this immersion, the films were extracted from the water and subjected to a drying process in an oven set at 45 °C for an additional 24 h to ascertain the final weight. The solubility was then computed employing Equation (4):

$$\text{Variation in mass } (\%) = \frac{(Mi - Mf)}{(Mi)} \cdot 100 \quad (4)$$

where Mi is the initial weight of the film and Mf is the final weight of the film after immersion in water.

Water Vapor Permeability Rate (WVPR)

The properties of water vapor permeability were scrutinized to evaluate the implications of the reinforcements for the barrier attributes of the material, conducted in accordance with the ASTM E 96/E standard [25]. Utilizing containers with circular apertures, each having an area of 0.0007 m^2, the films were positioned atop glass and situated within a desiccator containing silica at ambient temperature. The cumulative weight loss of the system was documented at 24 h intervals over a span of five days (represented as "G" in the subsequent equation). This series of measurements was executed in duplicate for each formulation, and the Water Vapor Permeability Rate (WVPR) was derived by applying Equation (5) [24],

$$\text{TPVA} = \frac{G}{tA} \tag{5}$$

where G corresponds to the weight variation, t is the duration of the test every 24 h, and A is the test film area (0.0007) in m^2. Thus, the final unit of WVPR is g/m^2 in 24 h [26].

Optical Microscopy (OM)

The morphological characteristics and the distribution of the reinforcements within the PVA matrix were assessed through optical microscopy analysis. Imagery was captured utilizing a trinocular stereomicroscope, model 06-KTESD5000, of the Laborama brand, employing a 4× zoom magnification.

Thermogravimetry (TGA)

In order to investigate whether there was interference in the thermal stability of the films with reinforcement compared to the PVA film (Pure), the thermogravimetric analysis (TGA) was performed. The conditions of the equipment were the same as are described in Section 2.5.1.

Differential Scanning Calorimetry (DSC)

The melting temperature of the films was investigated through DSC analysis, employing the TA Instruments model Q2000, under a nitrogen atmosphere maintaining a constant flow of 50 mL/min. The films were subjected to a temperature elevation from ambient to 200 °C at a progression rate of 10 °C/min, and were sustained at this temperature for a duration of three min. Subsequently, the samples were reverted to a temperature of 30 °C at a cooling rate of 10 °C/min.

Evaluation of Biodegradation in Soil

For the preparation of soil, a concoction was formulated using 1.4 kg of beach sand, 1.4 kg of horse manure dried for a duration of 48 h, and 1.4 kg of equal parts of fertile soil. This mixture was subsequently blended with the aid of a shovel and moisturized to maintain soil hydration. Prior to the insertion of the films, the soil mixture was allowed a maturation period of three months within a container, aligning with the stipulations of ASTM G 160-03 [27]. The biodegradation rates of the films were then ascertained by examining the mass loss, computed via Equation (6) [28]:

$$\text{Mass Loss } (\%) = \frac{(\text{Mi} - \text{Mf})}{(\text{Mi})} \cdot 100 \tag{6}$$

where Mi is the initial mass and Mf corresponds to the final mass.

For the analysis, soil, already matured, was allocated in plastic containers, following which the films were trimmed to dimensions of 5 × 5 cm. The films, sorted according to each composition type, were designated to individual containers, subsequently placed in an oven

set at 30 °C, and thereafter extracted at predetermined intervals of 15, 30, 45, and 60 days. Following each interval, the films were cleansed and subjected to weighing procedures.

Tensile Test

The mechanical characterization for tensile properties was conducted utilizing a Dynamic-Mechanical Analyzer (DMA), model Q800TM, version 20.6.4, facilitated by TA Universal Analisys 2000 software version 4.5A Build 4.5.0.5. The analysis was executed at 25 °C, employing an 18 N load cell and administering a pre-load of 0.5 N, at a testing velocity of 3 N/min. Accordingly, the films were precision-cut to dimensions of 5 mm in width and 30 mm in length.

3. Results and Discussion

3.1. Characterization of Rice Husk, Cellulose and Nanocellulose

3.1.1. Fourier Transform Infrared Spectroscopy (FTIR)

The Fourier Transform Infrared Spectroscopy (FTIR) technique was employed to discern alterations in the chemical structure of the pristine rice husk, cellulose, and nanocellulose subsequent to the applied treatments.

Figure 2 delineates the FTIR outcomes for the examined samples. A notably intense region between 3321 cm^{-1} and 3376 cm^{-1} is observable across all samples, the spectra of which are attributed to the axial elongation of hydroxyl groups (O-H), originating from intramolecular hydrogen bonds typical of Type I cellulose [29]. The spectrum identified in the 2907 cm^{-1} region is ascribed to symmetric bond elongation (C-H) vibrations. The regions at 898 cm^{-1} and 1035 cm^{-1} signify cellulose β-glycosidic bonds, corresponding to stretching vibrations (C-O-C). Herein, a pronounced increase in intensity is perceivable for cellulose and nanocellulose samples, indicative of enhanced crystalline stability in the material structures post-treatments [8].

The band positioned at 1719 cm^{-1} is correlated with the stretching vibrations of carbonyl groups (C=O), inherent to hemicellulose. The 1438 cm^{-1} band is indicative of the structural configuration of lignin's aromatic rings, represented by stretches (C=C). Consequently, cellulose and nanocellulose exhibit a diminution in the intensities of these peaks upon treatment, suggesting a reduction in the hemicellulose and lignin constituents within the treated samples [30].

In the nanocellulose specimen, an amplified intensity in the regions of 1250 cm^{-1} and 818 cm^{-1} is notable, linked to the stretching vibrations of (C-O-S) and (S=O). This transformation denotes the incorporation of acid sulfate groups onto the fiber surface, substantiating the efficacy of the sulfuric acid hydrolysis treatment [31].

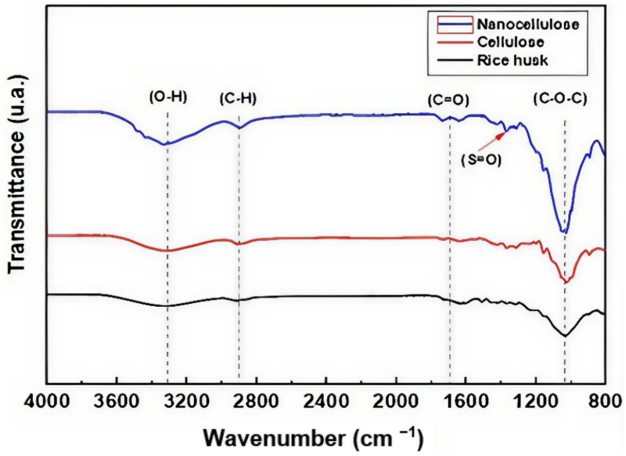

Figure 2. FTIR spectra for rice husk, cellulose and nanocellulose.

3.1.2. X-Ray Diffraction (XRD)

X-ray diffraction (XRD) analyses were performed using a Shimadzu XRD-6000 diffractometer (at the Barueri, SP/Brazil). The scanning parameters included a scanning rate of 0.5°/min over a 2θ range of 10° to 90°, with a wavelength (λ) of 1.541 Å. The equipment was operated at 40 kV and 40 mA.

The X-ray diffractograms facilitated the exploration and verification of the chemical structures of the rice husk, cellulose, and nanocellulose samples, as illustrated in Figure 3.

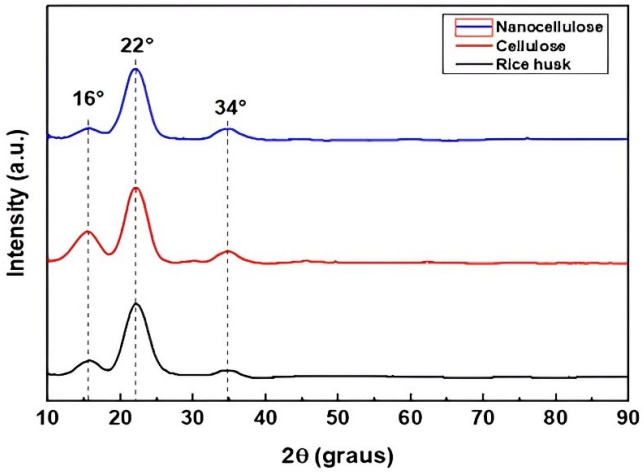

Figure 3. XRD of rice husk, cellulose and nanocellulose.

The depicted curves reveal the occurrence of three distinctive peaks for each sample, each with varying intensities, correlating to the type I crystalline structure of native cellulose.

The diffraction signals showcase intensities at 2θ of 16°, pertaining to the 110 plane, 22°, attributed to the 002 plane, and 34°, corresponding to the 004 plane [8]. In analyzing the diffractograms, it is observable that all samples exhibit a semi-crystalline structure, with peaks at 16° representing the amorphous region and those at 22° denoting the crystalline region, typical of such materials [32].

Furthermore, a diminished peak intensity is discernible in the 16° region for the nanocellulose sample, a decrease attributable to the extraction of amorphous constituents like lignin and hemicellulose inherent in the rice husk structure. Nonetheless, the enhancement in crystallinity and the reduction in amorphous components are conjectured to augment film attributes upon their integration into the polymer matrix [33].

The diffractograms made it possible to calculate the crystallinity index for the studied samples, and the results are presented in Table 1.

Table 1. Crystallinity index values.

Samples	Crystallinity Index (%)
Rice husk	46%
Cellulose	62%
Nanocellulose	74%

It is discernible that there was an elevation in the crystallinity index of the cellulose and nanocellulose samples subsequent to the treatments, attaining values of 62% for cellulose and 74% for nanocellulose. This increment indicates the successive diminution of the amorphous components inherent in the fiber structure, thereby validating the efficacy of the procedures applied to the fiber.

As articulated by Rashid and Dutta [8], the enhancement in the crystallinity index of processed materials, in contrast to their unprocessed counterparts, is attributed to the

reordering of crystals into configurations of superior orientation, as well as due to the elimination of amorphous substances such as lignin and hemicellulose.

3.1.3. Thermogravimetry (TGA)

The thermal resilience of rice husk (RH), cellulose (CE), and nanocellulose (NC) was scrutinized utilizing mass loss curves in correlation with temperature (TGA) and the derivative of mass alteration (DTG), as depicted in Figure 4.

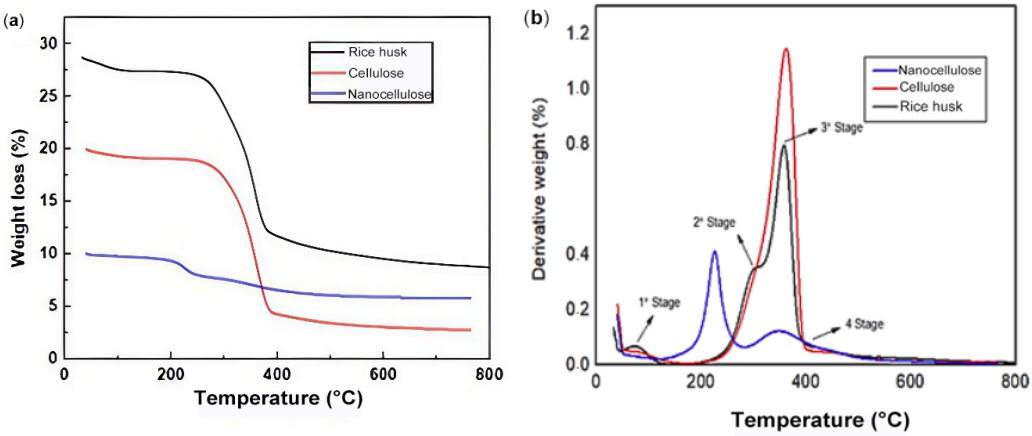

Figure 4. Thermogravimetry analysis—(**a**) TGA and (**b**) DTG curves of rice husk, cellulose and nanocellulose samples.

The initial stage, ranging between 25 °C and 123 °C, signifies an early mass reduction due to the evaporation of water and other volatile extractives. The second stage, manifest solely in the rice husk sample, transpires between approximately 232 °C and 300 °C, arising from the decomposition of hemicellulose. The absence of this stage in the cellulose and nanocellulose samples substantiates a reduction in amorphous material following the implemented treatments [34].

Evolving into the third stage, occurring in the range of 300–355 °C, the behavior is synonymous with the degradation of cellulose, marked by dehydration and the decomposition of its glycosidic units. The ensuing fourth stage, occurring between 400 °C and 600 °C, is indicative of the degradation of lignin and silica, resulting in the breakdown of residual carbon compounds [32].

While meticulously examining the TGA and DTG curves, a nuanced reduction in the thermal stability of nanocellulose becomes evident, occurring around 220 °C and corresponding to the third stage, indicative of a comparative analysis with rice husk and cellulose samples. This subtle decline is interpreted as the consequence of the incorporation of sulfate groups from sulfuric acid onto the surface of nanocellulose, facilitating the degradation of the material at relatively lower temperatures [35,36].

3.2. Films Characterization

3.2.1. Thickness, Weight and Density

With the data accumulated for thickness, weight and density, as outlined in Table 2, it was possible to explore the potential changes in film properties due to the incorporation of reinforcements.

Thickness stands as a crucial attribute requiring meticulous evaluation, as it governs the dispersion control of the reinforcement within the matrix.

Table 2. Obtained thickness, weight and density values for the films.

Samples	Thickness (mm)	Grammage (g/cm^{-2})	Density (g/cm^{-3})
PVA	0.16 ± 0.02	0.020 ± 0.003	1.25 ± 0.15
PVA/RH	0.22 ± 0.04	0.031 ± 0.002	1.41 ± 0.05
PVA/CE	0.20 ± 0.03	0.028 ± 0.001	1.40 ± 0.03
PVA/NC	0.18 ± 0.03	0.023 ± 0.002	1.27 ± 0.06

Subsequently, thickness variability bears significant implications in relation to diverse film characteristics, including mechanical, permeability, and optical properties. An assessment of Table 2 reveals a progressive increase in thickness values with the incorporation of reinforcement within the matrix. The film exhibiting the greatest thickness was the PVA fortified with rice husk, and the one with minimal thickness was pure PVA; this increment is rationalized by the granule dimensions of the rice husk and its subordinate dispersion in the PVA matrix. In contrast, the PVA film fortified with nanocellulose did not manifest a substantial thickness elevation compared to pure PVA film, attributed to its proficient dispersion within the matrix, ensuring optimal homogeneity between matrix and reinforcement [37].

Table 2 additionally enumerates the weight specifications of the films; this attribute is intricately linked to the mass of the material, and hence, can significantly impact the mechanical characteristics of the films. It is noteworthy that the PVA film fortified with rice husk manifested the highest weight values in comparison to its counterparts, a phenomenon resulting from the integration of untreated rice husk in natura form, inducing larger particles and challenging distribution within the matrix, consequently contributing to this weight augmentation [38].

Density, being interconnected with the weight and thickness of the films, plays a pivotal role in shaping the barrier and mechanical attributes of the material. An examination of the density data presented in Table 2 indicates that the PVA film with nanocellulose does not exhibit a considerable deviation in density values compared to the pure PVA film. This finding is ascribed to the interaction dynamics between PVA and nanocellulose, culminating in a structure that is more compact and less dense. Conversely, films reinforced with rice husk and cellulose illustrated a significant increase relative to the pure PVA film, attributed to the inferior dispersion capability of these materials within the matrix [39].

3.2.2. Transparency

The addition of polyvinyl alcohol gives the material important properties for packaging applications, such as excellent transparency and flexibility [23].

Figure 5 illuminates the aesthetic qualities of the films, wherein both pure PVA and PVA/nanocellulose films are discerned to exhibit sleek and uniform surfaces with negligible roughness. The excellent performance of the nanocellulose-reinforced film is due to the effective dispersion of nanocellulose within the PVA matrix, which is facilitated by the interaction and particle size.

Figure 5. Evaluation Transparency.

This synergy fosters robust adhesion between the nanocellulose and the matrix, rendering transparency attributes analogous to those observed in pure PVA films. Lee et al. [23] have similarly reported no alterations in the transparent properties of PVA upon the integration of nanocellulose.

Conversely, films fortified with rice husk and cellulose presented a cloudiness over the symbols coupled with a textured surface, resulting in films characterized by diminished visibility. These observations highlight the challenges in dispersing these materials within the PVA matrix, causing agglomerates that may reduce the films' mechanical properties [22].

3.2.3. Solubility

Polyvinyl alcohol, despite its advantages, faces limitations in humid environments, restricting its application mainly to areas with controlled temperatures.

Therefore, probing into the films' performance in aqueous settings becomes pivotal. The elucidations pertaining to the solubility of the films are depicted in Figure 6.

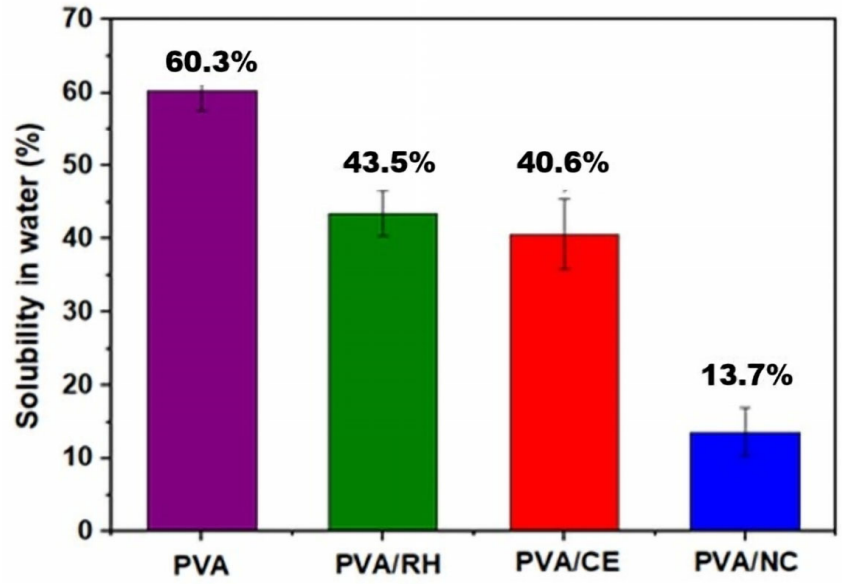

Figure 6. Percentage of solubility of PVA, PVA/RH, PVA/CE and PVA/NC films.

It is discernible that the pristine PVA film exhibited the most pronounced aqueous solubility, around 60.3%. This tendency is ascribed to its inherent hydrophilic nature and its propensity for high solubility in water, facilitated by the presence of hydroxyl groupings within its structure.

This promotes molecular penetration into the matrix, corroborating its susceptibility to hydrolytic degradation [40]. Conversely, it is observed that the incorporation of reinforcements decreases the solubility of PVA to 43.5% for the film fortified with rice husk and 40.6% for the cellulose-reinforced film, rendering these films more resistant to water relative to the pure PVA film due to the water-insoluble nature of these materials [41].

Regarding the nanocellulose-reinforced PVA film, a diminution in solubility is noted, with a recorded value of 13.7%. This phenomenon is linked to the diminution of accessible hydroxyl groupings within the PVA structure post-nanocellulose incorporation, resulting in the formation of a physical barrier within the film's structure, constraining chain mobility, and thereby conferring enhanced retention against the infiltration of water molecules. Such improved performance is pivotal for extending the shelf life of food products within packaging exposed to unregulated humidity conditions [22].

Patel and Joshi [38] documented analogous reductions in water solubility for PVA films augmented with nanocellulose derived from banana agricultural residue. They

recognized that films containing 1 wt. % of reinforcement exhibited a solubility reduction of approximately 2.04% in contrast to the pristine PVA film—a trend consistent with films comprising 2 wt. % and 5 wt. % of nanocellulose. This is rationalized by the crystalline nature of nanocellulose and the intermolecular forces established between the matrix and the reinforcement.

Noshirvani et al. [42] developed films incorporating PVA, starch, and cellulose nanocrystals, noting a decrease in film solubility coinciding with the incorporation of cellulose nanocrystals. This was substantiated by the formation of hydrogen bonds amongst the hydroxyl groups inherent in PVA, starch, and cellulose nanocrystals, facilitating a three-dimensional network that stabilized chain movement, thereby reducing water absorption for the fortified films.

3.2.4. Water Vapor Permeability Rate (WVPR)

The evaluation of Water Vapor Permeability Rate (WVPR) is crucial for materials destined for packaging applications. This assessment is instrumental in determining the extent of water transferred by the film, which is pivotal since ideal films should effectively shield products from external agents, translating to lower WVPR values.

Table 3 illustrates the variations in mass loss and transmission rates as water molecules traverse through the films over a 120 h period. It is observed that the introduction of reinforcements to the PVA matrix causes a decrement in both mass loss and WVPR values. This implies that the films incorporating reinforcements exhibit greater resistance to water molecule penetration compared to the pristine PVA film.

Table 3. Calculated values of mass loss and water vapor permeability rate of the films.

Samples	Weight Loss (g/120 h)	WVP ($g/m^2 \cdot 120$ h)
PVA	0.28 ± 0.12	410 ± 60
PVA/RH	0.27 ± 0.10	392 ± 40
PVA/CE	0.25 ± 0.09	357 ± 50
PVA/NC	0.23 ± 0.14	339 ± 33

In the context of nanocellulose-augmented samples, the mass loss registered was 0.237 g, indicative of the lowest water vapor transmission rate relative to the other variants. This outcome implies a harmonious interaction between nanocellulose and PVA, stemming from their mutual affinity attributed to the presence of hydroxyl groups. This affinity facilitates the formation of a hydrogen barrier obstructing water molecule passage, resulting in an enhancement of around 17% in the film's barrier properties compared to the unaltered PVA film [43]. It can be inferred, thus, that the integration of reinforcements into the matrix correlates with a diminished water vapor transmission rate.

Therefore, as a reinforcement is introduced into the PVA matrix, the water vapor transmission rate decreases.

In a study conducted by Srivastava et al. [44], PVA films were fabricated and reinforced with varying concentrations of nanocellulose—0.1, 0.5, 1.3, and 5%. The findings reveal a decline in the permeability of the films as nanocellulose was integrated, enhancing the barrier properties by approximately 29.7% when compared to the pure PVA films. Analogously, Espinosa et al. [45] incorporated nanocellulose extracted from wheat straw, both with and without lignin, into a PVA matrix in their research. It was observed that the introduction of nanocellulose led to a reduction in permeability values, creating a physical barrier that obstructs moisture passage, irrespective of the type of nanocellulose utilized.

3.2.5. Optical Microscopy (OM)

In previous studies conducted by the same research group, scanning electron microscopy (SEM) and transmission electron microscopy (TEM) analyses were performed to investigate the morphology and dispersion of nanocellulose in similar polymer matrices. These studies, described in [14], demonstrated that the nanocelluloses exhibited a uniform needle-like morphology, with nanometric dimensions and reduced aggregation compared to the initial fibers. Furthermore, the removal of amorphous components, such as lignin and hemicellulose, contributed to the production of well-defined cellulose nanocrystals (CNCs) with higher crystallinity and potential to enhance the properties of polymer nanocomposites due to their large surface area and exposed hydroxyl groups, which favor matrix–reinforcement interaction.

In addition, the production and characterization of nanocellulose in the present study were inspired by the methodology described by Zhang et al. [5], who successfully extracted nanofibrillated cellulose (NFC) from Enteromorpha prolifera with a diameter of 20–40 nm, a length of several microns, and a crystallinity index of 57.2%. These characteristics enabled its effective integration with polyvinyl alcohol (PVA) matrices, improving mechanical and barrier properties. Based on these findings, we assumed the successful production of nanocellulose in our work and proceeded with similar characterization techniques to confirm its properties. This comparison underscores the alignment of our results with those of Zhang et al. while exploring potential advancements in the application of nanocellulose as a reinforcing agent.

In the present study, optical microscopy was employed as a complementary approach to observe the morphology and dispersion of the reinforcements in the PVA matrix, aiming to correlate these results with the functional properties of the developed films.

The images secured through the stereomicroscope with 4× magnification are illustrated in Figure 7.

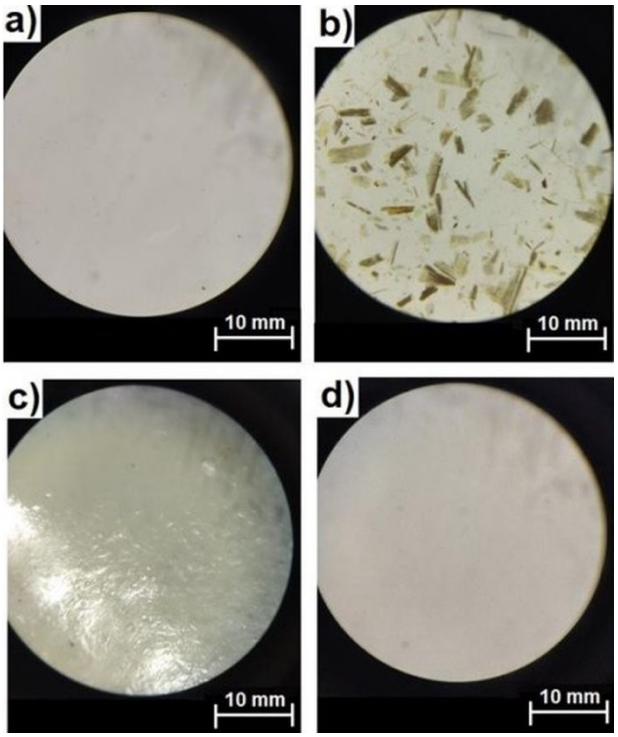

Figure 7. Microscopy images of: (**a**) PVA, (**b**) PVA reinforced with rice husk, (**c**) PVA reinforced with cellulose, (**d**) PVA reinforced with nanocellulose.

Figure 7a delineates that the pure PVA film features a smooth and uniform surface, thereby exhibiting an absence of defects such as bubbles or fissures.

Contrarily, the PVA film fortified with rice husk, as depicted in Figure 7b, distinctly displays fibers of uneven configurations throughout its structure, accompanied by clusters and void spaces, a representation of suboptimal dispersion.

Figure 7c illustrates the texture of the PVA films bolstered with cellulose, revealing a coarse surface interspersed with bubbles and displaying uneven distribution. These imperfections can potentially compromise the mechanical properties of the films. On the other hand, the PVA films integrated with nanocellulose, as seen in Figure 7d, reflect properties strikingly similar to those of the pure PVA film. They showcase a smooth, immaculate surface, a feature ascribed to the smaller scale of nanocellulose relative to cellulose and rice husk reinforcements, facilitating enhanced synchronization between the reinforcement and the matrix [45].

Wang et al. [46] also explored PVA films strengthened with cellulose nanofibers derived from rice straw in their research. They too discerned enhanced dispersion and uniformity in the films compared to those fortified with cellulose microfibrils. Moreover, the integration of cellulose nanofibers not only augmented the mechanical properties, but also elevated the transparency of the films.

3.2.6. Thermogravimetry (TGA)

The execution of TGA analyses was pivotal to exploring how the infusion of reinforcements could potentially alter the thermal stability of the films. The curves depicting mass loss relative to temperature (TGA) and the derivative of mass variation (DTG) for the films are illustrated in Figure 8.

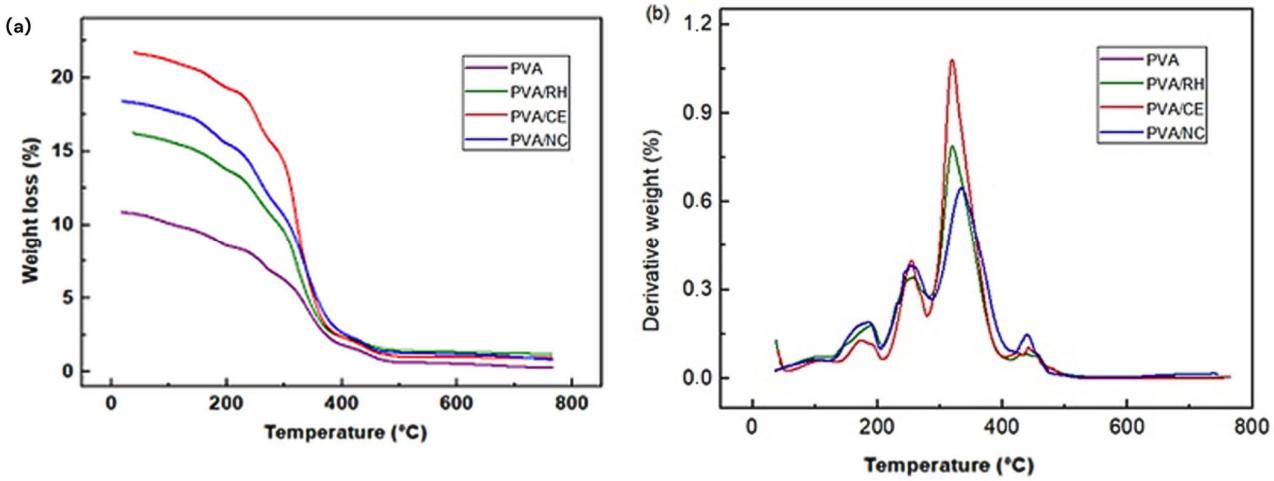

Figure 8. Thermogravimetry analysis—(**a**) TGA and (**b**) DTG curves of the films.

Surveying the TGA and DTG curves reveals that every film underwent three principal phases of mass reduction. The initial phase, ranging between 50 °C and 130 °C, is ascribed to the decomposition of substances on the films' surface and the evaporation of entrained moisture [47]. Following this, a second phase emerges between approximately 287 °C and 370 °C, linked to the decomposition of oxygen-bearing functional groups in the PVA structure and the liberation of volatile compounds contained within the films. A close inspection of the DTG curves displayed in Figure 8b discloses a marginal enhancement in the thermal resilience of both PVA and nanocellulose-augmented PVA films compared to their rice husk- and cellulose-reinforced counterparts.

Such outcomes intimate that integrating this type of reinforcement with the polymer matrix could manifest thermal characteristics analogous to those of uncontaminated PVA without markedly impacting its thermal robustness [48].

Conclusively, the last phase, unfolding between 425 °C and 487 °C, pertains to the decomposition of carbonaceous compounds and the breakdown of functional entities inhabiting the principal chain of polyvinyl alcohol [49].

3.2.7. Differential Scanning Calorimetry (DSC)

DSC analysis was utilized to scrutinize the thermal attributes of the films, yielding insights into melting temperature (Tm), crystallization temperature (Tc), enthalpy alteration (ΔH), and the crystallinity degree (Xc). The heating and cooling thermograms are depicted in Figure 9.

The parameters derived from the DSC assessments are cataloged in Table 4.

Table 4. Data obtained from the DSC curves.

Samples	Tm (°C)	Tc (°C)	ΔH (J/g)	Xc (%)
PVA	163	126.14	13.92	8.73
PVA/RH	164	122.34	12.94	8.11
PVA/CE	170	134.15	11.58	7.26
PVA/NC	165	129.14	11.39	7.14

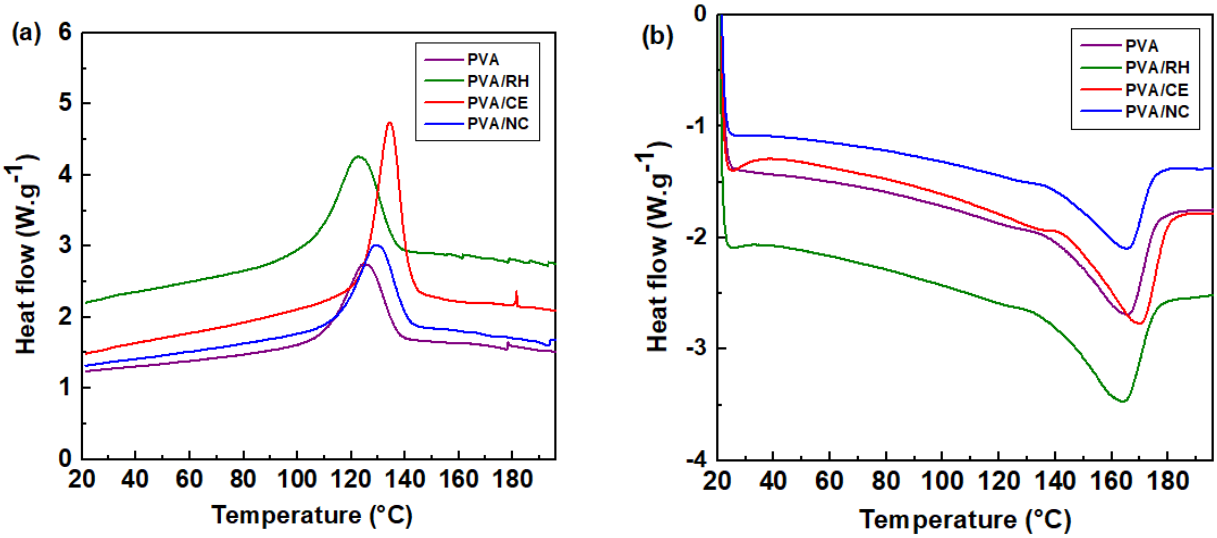

Figure 9. DSC curves—(**a**) cooling for the films and (**b**) heating for the films.

The films predominantly demonstrated analogous onset melting temperatures, around 140 °C, with negligible alterations. This occurrence is linked to the disruption of intermolecular bonds in the films' hydroxyl groups. Pertaining to the melting temperature, a modest augmentation is discernible in the values for the films with filler integration, notably for the cellulose-reinforced film, in comparison to the pristine PVA film. This observation could be correlated with the interaction proficiency between PVA and the reinforcements, thereby illustrating the enhancement of the films' thermal stability [42,50].

Following the integration of the reinforcements, a surge in Tc was manifested, especially in the cellulose-inclusive film, displaying approximately 134.15 °C in contrast to the pure PVA's 126.14 °C. This modification in Tc could be related to the impact of the reinforcements on the matrix, serving as nucleation facilitators, hence fostering an elevation in crystallization temperature [51,52].

Moreover, the Xc values, deduced by interpreting the DSC curves via the applicable equation, witnessed a gradual decline. This can potentially be ascribed to the reinforcements instigating the formation of new hydrogen bonds with PVA molecules, disrupting the regular arrangement of the molecular chains, and subsequently impeding PVA's crystallization [53].

3.2.8. Evaluation of Biodegradation in Soil

The appraisal of the material's biodegradability in soil is critical when contemplating its deployment for packaging solutions. Soil biodegradation is influenced by various factors like humidity, the activity of microorganisms, and the presence of fungi and bacteria within the soil [54]. In this research, the biodegradability of the films was assessed based on mass loss at intervals of 0, 15, 30, 45, and 60 days of burial in soil, with the outcomes displayed in Table 5.

Table 5. Average in grams of film weights over time.

Samples	Day 0	Day 15	Day 30	Day 45	Day 60
PVA	0.432	0	0	0	0
PVA/RH	0.494	0	0	0	0
PVA/CE	0.452	0	0	0	0
PVA/NC	0.444	0.267	0.065	0.037	0

The only film displaying resilience to the biodegradation examination was the one reinforced with nanocellulose. Despite the hydrophilic nature of both PVA and nanocellulose, the incorporation of nanocellulose escalated the film's resistance to biodegradation. Nevertheless, despite its slowed degradation rate, the nanocellulose-infused film experienced a 100% mass loss before the completion of 60 days, illustrating a commendable outcome relative to conventional packaging materials.

This performance echoes previous solubility findings, where nanocellulose-reinforced films exhibited reduced solubility levels, signifying that the integration of nanocellulose enhances the polymer's resilience in humid conditions.

These results can be credited to the ability of the PVA matrix and nanocellulose to establish hydrogen bonds, creating a compact and dense three-dimensional configuration, and generating a convoluted route within the material. This intricate structure impedes microbial activities and minimizes water molecule penetration into the material, thereby constraining available space within the structure and reducing interface gaps between PVA and nanocellulose [5,55].

The data compiled in Table 5 facilitate the calculation of the percentage of mass loss subsequent to each period of sample retrieval, although this was solely applicable to the film fortified with nanocellulose. In the initial 15 days, a substantial weight reduction of 39.8% was recorded. In the following days (30 and 45), the degradation increased to 85.3% and 91.6%, respectively, due to water molecules and microorganisms penetrating the film structure, reducing its strength. Consequently, after 45 days, the moisture in the soil led to the complete dissolution of the nanocellulose film [56].

Moreover, alterations in the visual characteristics of the nanocellulose-reinforced PVA film over the 0-, 15-, 30-, and 45-day intervals were discernible, as illustrated in Figure 10. The images conspicuously depict a sustained reduction in film mass, concluding the 60-day period with no remnants of film residues observable.

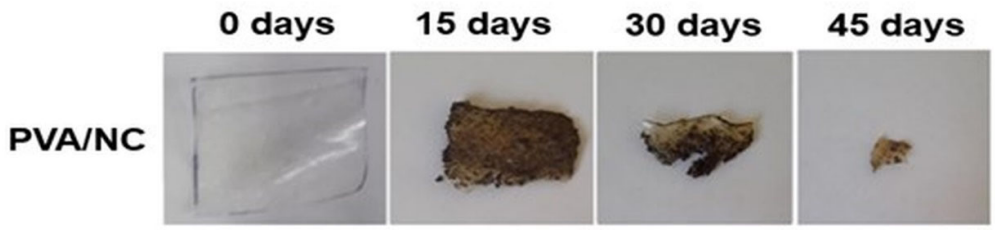

Figure 10. Evaluation of the visual appearance of the PVA/NC film after the biodegradation test.

Ong et al. [57] explored the soil biodegradability of PVA matrix films bolstered with 3, 5, and 10 wt. % by mass of various reinforcements. The reinforcements included microcrystalline cellulose, cellulose nanocrystals extracted from palm fiber, and commercial nanocrystals. They observed that the films exhibited a rapid rate of degradation; all the films underwent complete degradation after just 7 days of being buried in the soil.

The difference observed in degradation time between this study (more than 45 days) and the aforementioned study (7 days) can be attributed to several factors, such as the nature of the reinforcement, the process of obtaining nanocellulose and the experimental biodegradation conditions. While the previous study used commercial cellulose nanocrystals and higher concentrations, in this work, the nanocellulose was obtained from rice husk, an abundant agro-industrial residue, which can influence the structure and interaction of the reinforcement with the PVA matrix. The greater stability observed is due to the formation of a dense three-dimensional network between PVA and nanocellulose through hydrogen bonds, which limits water penetration and microbial activity [58,59].

This result reinforces the novelty of the present study, as it demonstrates that the use of nanocellulose extracted from agro-industrial waste can not only improve the mechanical and barrier properties of the film, but can also prolong its resistance under degradation conditions, making it more suitable for applications in packaging with greater durability, without compromising its final biodegradability.

3.2.9. Tensile Strength Test

Determining the mechanical properties of materials is critical, especially when understanding the interaction between reinforcement and matrix to ensure superior mechanical performance and uphold the product's integrity. Figure 11a illustrates the results for Young's modulus, while Figure 11b displays the values for tensile strength of the samples under consideration.

Examining Figure 11a, a progressive escalation in the elastic modulus is evident upon the integration of reinforcements into the PVA matrix. The elastic modulus relates to the material's rigidity; thus, a higher modulus denotes increased stiffness [60]. This observation implies that films fortified with nanocellulose showcased the best elastic modulus, marking a noteworthy enhancement in comparison to the unmodified PVA film. This augmented mechanical resilience is attributed to the potent interaction and hydrogen bonding between PVA and nanocellulose, fostering optimal affinity and the homogeneous dispersion of nanocellulose within the PVA matrix [45]. This enhancement in modulus and overall mechanical strength demonstrates the successful synergism between the matrix and the reinforcement, crucial for applications requiring elevated mechanical stability.

When it comes to the tensile strength of the films, Figure 11b reveals that the pure PVA film acquired a value of 2.5 MPa, whereas the films reinforced with rice husk and cellulose registered lower values. More specifically, the rice husk-reinforced film (PVA/RH) exhibited a value of 1.7 MPa and the cellulose-reinforced film (PVA/CE) yielded 1.45 MPa. This suggests a non-uniform dispersion of the reinforcement within the matrix, resulting in uneven tension transfer across the material. Conversely, the nanocellulose-incorporated

film demonstrated an enhancement, reaching 3.24 MPa. This improvement is correlated to the robust interaction between the hydroxyl groups in nanocellulose and PVA, engendering hydrogen bonds, and thus establishing strong interfacial adhesion and a better tension distribution throughout the material [50,61].

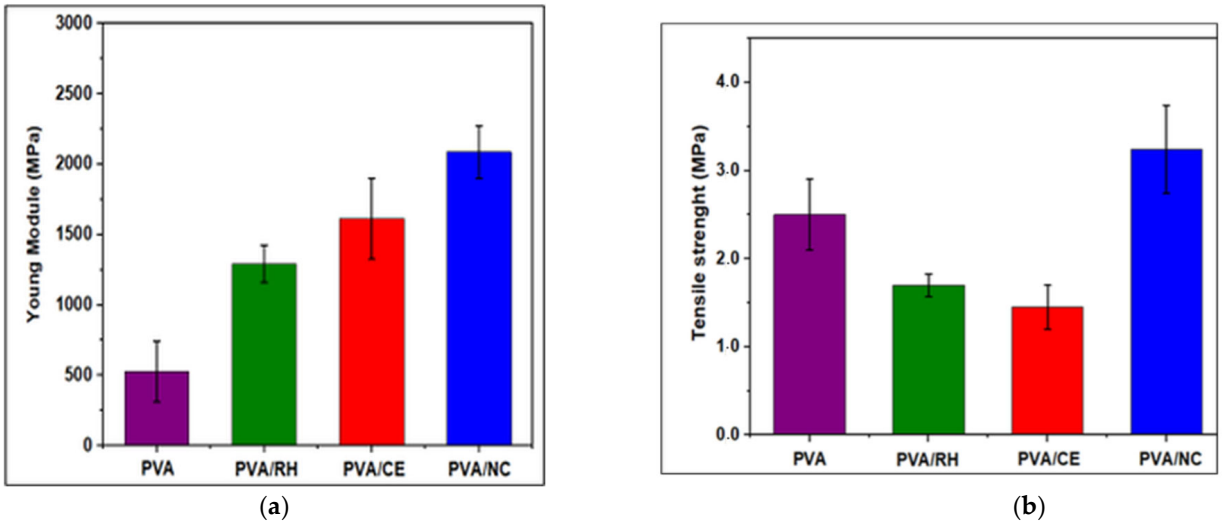

Figure 11. Graph of the average values of the Young's Modulus (**a**) and tensile strength (**b**) of the films.

Similar findings were noted by Ong et al. [49] when assessing the mechanical performance of PVA films reinforced with cellulose nanocrystals. These nanocrystals, extracted from palm oil fiber, were used in proportions of 3, 5, and 10 wt. % by mass. They reported augmented tensile strength and elasticity modulus, particularly in films containing 5 wt. % cellulose nanocrystals, relative to the pure PVA film.

The mechanical and barrier properties obtained align with recent findings on PVA/nanocellulose composites, where the addition of nanocellulose improved tensile strength and reduced WVTR [62].

In summary, rice husk waste is a significant byproduct of rice production in Rio Grande do Sul, presenting both challenges and opportunities for sustainable management and utilization.

Furthermore, Srivastava et al. [44] elucidated that incorporating 3 wt. % by mass of nanocellulose into the PVA matrix led to a 14.3% increment in the films' tensile strength relative to pure PVA. This enhancement is principally attributed to the presence of hydroxyl bonds within the material's structure, fostering a strongly intertwined three-dimensional network. This network ensures superior interfacial adhesion between the reinforcement and the matrix, thereby elevating the tensile strength of the films. This structural synergy and increased interaction between matrix and reinforcement underscore the potential use of nanocellulose in enhancing the mechanical properties of polymer composites.

4. Conclusions

This study established that the employed methodologies for cellulose extraction and nanocellulose acquisition were efficacious, as substantiated by the FTIR and XRD analyses. These analyses reveal alterations in the chemical structures of the fibers and a diminishment in amorphous constituents after the applied treatments. The TGA analysis pertaining to the fibers' thermal properties disclosed a decrement in the thermal stability of the nanocellulose sample. Evaluations of the films' thickness, grammage, and density revealed augmented values for those integrated with reinforcements in the PVA matrix.

The PVA/nanocellulose film demonstrated the lowest solubility, showcasing enhanced water resilience in comparison to its counterparts. Concurrently, there was a notable reduction in the water vapor permeability rate for films integrated with reinforcements, primarily those strengthened with nanocellulose. The examination of optical microscopy images highlighted suboptimal dispersion, evident voids, and agglomerations in films fortified with cellulose and rice husk. This outcome is attributed to particle size disparities, leading to the non-uniform dispersion of reinforcements within the matrix. Conversely, films bolstered with nanocellulose displayed optimal dispersion and characteristics analogous to pure PVA films.

For thermal properties, the TGA results showed slight instability in the cellulose-reinforced film, while DSC analysis revealed minimal differences between reinforced and pure PVA films.

The obtained results illuminate the advantageous impact of nanocellulose incorporation within the PVA matrix. Nanocellulose not only elevated the water and biodegradation resistance, but also preserved the inherent flexibility and transparency, of the films, all while enhancing their mechanical properties. Such enhancements make nanocellulose-fortified materials a practical and beneficial alternative for applications like quick-use packaging, including films for dry food trays and seedling planting bags, consolidating them as promising solutions in the realm of sustainable packaging. This aligns with the growing emphasis on environmentally friendly alternatives, reflecting an integration of innovation and sustainability in material science.

This study has significant advantages over similar research. One of the main pros is the sustainable use of agro-industrial waste, such as rice husks, which promotes the reuse of discarded materials, reducing environmental impacts and costs. In addition, the films developed showed notable improvements in mechanical and functional properties, such as greater tensile strength and modulus of elasticity, and a reduction in solubility and water vapor permeability. Another positive point is the greater stability of the films in biodegradation tests, with prolonged degradation for more than 45 days, which makes them more suitable for practical applications in packaging.

On the other hand, there are some cons to consider. Processing nanocellulose involves intensive chemical steps, such as acid hydrolysis, which can be economically costly and generate additional waste. In addition, difficulties have been observed in the uniform dispersion of larger-scale reinforcements, such as cellulose and rice husk, which have a negative impact on the optical and mechanical properties of the films. Finally, the scalability of the process on a large scale is still a challenge, requiring further studies to make industrial production of the developed materials feasible.

In addition, by using agro-industrial waste, such as rice husks from Rio Grande do Sul, Brazil's largest rice producer, this research helps to solve the significant waste management challenges faced by the Brazilian agricultural sector. The recovery of this waste not only reduces environmental pollution and the costs associated with improper disposal, but also aligns with global sustainability commitments and the principles of the circular economy.

These points highlight the advances and limitations of the study, highlighting its innovative potential, but also pointing out the areas that require optimization for future commercial applications.

Author Contributions: G.M.C.: methodology, writing, data analysis, conceptualization, investigation, verification, roles/writing—original draft. M.W.B.: roles/writing—original draft, data analysis. A.A.R.: methodology. C.A.G.B.: methodology, writing—review and editing. T.C.F.: methodology. N.D.F.: review and editing. N.V.V.d.N. roles/review and editing. A.F.G.: methodology, data analysis. A.L.M.: supervision, methodology, data analysis, writing—review and editing. A.D.d.O.: supervision, methodology, data analysis, writing—review and editing. All authors have read and agreed to the published version of the manuscript.

Funding: This study was financed in part by the Coordenação de Aperfeiçoamento de Pessoal de Nível Superior—Brasil (CAPES)—Finance Code 001; the Federal University of Pampa—UNIPAMPA and the Department of Materials Engineering of Federal University of São Carlos (DEMa/UFSCar).

Data Availability Statement: The data presented in this study are available on request from the corresponding author.

Acknowledgments: The authors gratefully acknowledge the financial support from the Coordenação de Aperfeiçoamento de Pessoal de Nível Superior—Brasil (CAPES)—Finance Code 001, the Federal University of Pampa (UNIPAMPA), and the Department of Materials Engineering of the Federal University of São Carlos (DEMa/UFSCar).

Conflicts of Interest: The authors declare that they have no known competing financial interests or personal relationships that could have appeared to influence the work reported in this paper.

References

1. Xu, Y.; Liu, X.; Jiang, Q.; Yu, D.; Xu, Y.; Wang, B.; Xia, W. Development and properties of bacterial cellulose, curcumin, and chitosan composite biodegradable films for active packaging materials. *Carbohydr. Polym.* **2021**, *260*, 117778. [CrossRef] [PubMed]
2. Cazón, P.; Velázquez, G.; Vázquez, M. Characterization of bacterial cellulose films combined with chitosan and polyvinyl alcohol: Evaluation of mechanical and barrier properties. *Carbohydr. Polym.* **2019**, *216*, 72–85. [CrossRef]
3. Yazik, A.; Tukiran, N.A. Characterization of Polyvinyl Alcohol (PVA) as Antimicrobial Biocomposite Film: A Review. *Malays. J. Sci. Health Technol.* **2021**, *7*, 79–85. [CrossRef]
4. Garavand, Y.; Taheri-Garavand, A.; Garavand, F.; Shahbazi, F.; Khodaei, D.; Cacciotti, I. Starch-Polyvinyl Alcohol-Based Films Reinforced with Chitosan Nanoparticles: Physical, Mechanical, Structural, Thermal and Antimicrobial Properties. *Appl. Sci.* **2022**, *12*, 1111. [CrossRef]
5. Zhang, Z.; Liu, X.; Wang, H.; He, H.; Bai, R. Preparation and characterization of *Enteromorpha prolifera* nanocellulose/polyvinyl alcohol composite films. *Polym. Compos.* **2021**, *42*, 1712–1726. [CrossRef]
6. Ferrer, A.; Pal, L.; Hubbe, M. Nanocellulose in packaging: Advances in barrier layer technologies. *Ind. Crop. Prod.* **2017**, *95*, 574–582. [CrossRef]
7. Malucelli, L.C.; Lacerda, L.G.; Dziedzic, M.; da Silva Carvalho Filho, M.A. Preparation, properties and future perspectives of nanocrystals from agro-industrial residues: A review of recent research. *Rev. Environ. Sci. Bio/Technol.* **2017**, *16*, 131–145. [CrossRef]
8. Rashid, S.; Dutta, H. Characterization of nanocellulose extracted from short, medium and long grain rice husks. *Ind. Crop. Prod.* **2020**, *154*, 112627. [CrossRef]
9. de Souza, D.M.; Modolo, R.C.E.; dos Santos, E.A.; da Silva, J.L.; Sachetti, F.A.; Kappler, G.; Brehm, F.A.; Moraes, C.A.M. Evaluation of the properties of biochar obtained from rice husk for its application in agricultural soils. *Rev. AIDIS* **2023**, *16*, 398–417. [CrossRef]
10. Nadaleti, W.C.; Cardozo, E.; Bittencourt, J.; Pereira, P.; Santos, M.; Gomes, E.; Haertel, P.L.; Corrêa, É.K.; Vieira, B.M.; Rodrigues Junior, F.M. Hydrogen and electricity potential generation from rice husks and persiculture biomass in Rio Grande do Sul, Brazil. *Renew. Energy* **2023**, *216*, 118940. [CrossRef]
11. Thomas, J.; Patil, R.S.; Patil, M.; John, J. Addressing the Sustainability Conundrums and Challenges within the Polymer Value Chain. *Sustainability* **2023**, *15*, 15758. [CrossRef]
12. Gómez-Aldapa, C.A.; Velazquez, G.; Gutierrez, M.C.; Rangel-Vargas, E.; Castro-Rosas, J.; Aguirre-Loredo, R.Y. Effect of polyvinyl alcohol on the physicochemical properties of biodegradable starch films. *Mater. Chem. Phys.* **2020**, *239*, 122027. [CrossRef]
13. dos Santos, R.M.; Neto, W.P.F.; Silvério, H.A.; Martins, D.F.; Dantas, N.O.; Pasquini, D. Cellulose nanocrystals from pineapple leaf, a new approach for the reuse of this agro-waste. *Ind. Crop. Prod.* **2013**, *50*, 707–714. [CrossRef]
14. Bosenbecker, M.W.; Maron, G.K.; Alano, J.H.; Marini, J.; de Oliveira, A.D. Isolation of cellulose nanocrystals from Bambusa vulgaris pulp via physio-chemical approach. *Biomass- Convers. Biorefinery* **2022**, *14*, 14153–14162. [CrossRef]

15. Shapovalova, I.; Vurasko, A.; Petrov, L.; Kraus, E.; Leicht, H.; Heilig, M.; Stoyanov, O. Hybrid composites based on technical cellulose from rice husk. *J. Appl. Polym. Sci.* **2018**, *135*, 45796. [CrossRef]
16. Daniati, R.; Zulnazri, Z.; Hakim, L.; Hasbullah, S.A. Study of Cellulose Extraction from Robusta Coffee Husk Using NaOH Solution. *Int. J. Eng. Sci. Inf. Technol.* **2021**, *2*, 73–78. [CrossRef]
17. Hua, Y.L.; Harun, S.; Sajab, M.S.; Jahim, J.M.; Shah SS, M. Extraction of cellulose and microcrystalline cellulose from kenaf. *J. Kejuruter.* **2020**, *32*, 205–213. [CrossRef] [PubMed]
18. Kord, B.; Malekian, B.; Yousefi, H.; Najafi, A. Preparation and characterization of nanofibrillated Cellulose/Poly (Vinyl Alcohol) composite films. *Maderas-Cienc Tecnol* **2016**, *18*, 743–752. [CrossRef]
19. Segal, L.; Creely, J.J.; Martin, A.E., Jr.; Conrad, C.M. An Empirical Method for Estimating the Degree of Crystallinity of Native Cellulose Using the X-Ray Diffractometer. *Text. Res. J.* **1959**, *29*, 786–794. [CrossRef]
20. Ni, S.; Liu, N.; Fu, Y.; Bian, H.; Zhang, Y.; Chen, X.; Gao, H.; Dai, H. Laccase-catalyzed chitosan-monophenol copolymer as a coating on paper enhances its hydrophobicity and strength. *Prog. Org. Coatings* **2021**, *151*, 106026. [CrossRef]
21. Iewkittayakorn, J.; Khunthongkaew, P.; Wongnoipla, Y.; Kaewtatip, K.; Suybangdum, P.; Sopajarn, A. Biodegradable plates made of pineapple leaf pulp with biocoatings to improve water resistance. *J. Mater. Res. Technol.* **2020**, *9*, 5056–5066. [CrossRef]
22. Hiremani, V.D.; Sataraddi, S.; Bayannavar, P.K.; Gasti, T.; Masti, S.P.; Kamble, R.R.; Chougale, R.B. Mechanical, optical and antioxidant properties of 7-Hydroxy-4-methyl coumarin doped polyvinyl alcohol/oxidized maize starch blend films. *SN Appl. Sci.* **2020**, *2*, 1877. [CrossRef]
23. Lee, H.; You, J.; Jin, H.-J.; Kwak, H.W. Chemical and physical reinforcement behavior of dialdehyde nanocellulose in PVA composite film: A comparison of nanofiber and nanocrystal. *Carbohydr. Polym.* **2020**, *232*, 115771. [CrossRef] [PubMed]
24. Luchese, C.L.; Benelli, P.; Spada, J.C.; Tessaro, I.C. Impact of the starch source on the physicochemical properties and biodegradability of different starch-based films. *J. Appl. Polym. Sci.* **2018**, *135*, 46564. [CrossRef]
25. *ASTM E 96/E 96M-05*; Standard Test Methods For Water Vapor Transmission of Materials. American Society for Testing and Materials: Philadelphia, PA, USA, 2005.
26. Davletbaeva, I.M.; Dulmaev, S.E.; Sazonov, O.O.; Klinov, A.V.; Davletbaev, R.S.; Gumerov, A.M. Water vapor permeable polyurethane films based on the hyperbranched aminoethers of boric acid. *RSC Adv.* **2019**, *9*, 23535–23544. [CrossRef] [PubMed]
27. American Society for Testing and Materials. *ASTM G 160—Standard pratice for Evaluating Microbial Susceptibility of Nonmetallic Materials By Laboratory Soil Burial v. 14.04"*; American Society for Testing and Materials: Philadelphia, PA, USA, 2004.
28. Coelho, N.S.; Almeida, Y.M.B.; Vinhas, G.M. A biodegradabilidade da blenda de poli(β-Hidroxibutirato-co-Valerato)/amido anfótero na presença de microrganismos. *Polim. Tecnol.* **2008**, *18*, 270–276. [CrossRef]
29. de Souza, A.G.; Barbosa, R.F.S.; Rosa, D.S. Nanocellulose from Industrial and Agricultural Waste for Further Use in PLA Composites. *J. Polym. Environ.* **2020**, *28*, 1851–1868. [CrossRef]
30. Nang An, V.; Chi Nhan, H.T.; Tap, T.D.; Van TT, T.; Van Viet, P.; Van Hieu, L. Extraction of High Crystalline Nanocellulose from Biorenewable Sources of Vietnamese Agricultural Wastes. *J. Polym. Environ.* **2020**, *28*, 1465–1474. [CrossRef]
31. Zhao, G.; Du, J.; Chen, W.; Pan, M.; Chen, D. Preparation and thermostability of cellulose nanocrystals and nanofibrils from two sources of biomass: Rice straw and poplar wood. *Cellulose* **2019**, *26*, 8625–8643. [CrossRef]
32. Hafid, H.S.; Omar, F.N.; Zhu, J.; Wakisaka, M. Enhanced crystallinity and thermal properties of cellulose from rice husk using acid hydrolysis treatment. *Carbohydr. Polym.* **2021**, *260*, 117789. [CrossRef] [PubMed]
33. Guo, Y.; Zhang, Y.; Zheng, D.; Li, M.; Yue, J. Isolation and characterization of nanocellulose crystals via acid hydrolysis from agricultural waste-tea stalk. *Int. J. Biol. Macromol.* **2020**, *163*, 927–933. [CrossRef]
34. de Oliveira, J.P.; Bruni, G.P.; El Halal SL, M.; Bertoldi, F.C.; Dias AR, G.; da Rosa Zavareze, E. Cellulose nanocrystals from rice and oat husks and their application in aerogels for food packaging. *Int. J. Biol. Macromol.* **2019**, *124*, 175–184. [CrossRef]
35. Dai, H.; Ou, S.; Huang, Y.; Huang, H. Utilization of pineapple peel for production of nanocellulose and film application. *Cellulose* **2018**, *25*, 1743–1756. [CrossRef]
36. Naduparambath, S.; Jinitha, T.V.; Shaniba, V.; Sreejith, M.P.; Balan, A.K.; Purushothaman, E. Isolation and characterisation of cellulose nanocrystals from sago seed shells. *Carbohydr. Polym.* **2018**, *180*, 13–20. [CrossRef] [PubMed]
37. Collazo-Bigliardi, S.; Ortega-Toro, R.; Boix, A.C. Reinforcement of Thermoplastic Starch Films with Cellulose Fibres Obtained from Rice and Coffee Husks. *J. Renew. Mater.* **2018**, *6*, 599–610. [CrossRef]
38. Pego, M.F.F.; Bianchi, M.L.; Yasumura, P.K. Nanocellulose reinforcement in paper produced from fiber blending. *Wood Sci. Technol.* **2020**, *54*, 1587–1603. [CrossRef]
39. Kurt, A.; Kahyaoglu, T. Characterization of a new biodegradable edible film made from salep glucomannan. *Carbohydr. Polym.* **2014**, *104*, 50–58. [CrossRef] [PubMed]
40. Patel, B.H.; Joshi, P.V. Banana Nanocellulose Fiber/PVOH Composite Film as Soluble Packaging Material: Preparation and Characterization. *J. Packag. Technol. Res.* **2020**, *4*, 95–101. [CrossRef]
41. Jain, N.; Singh, V.K.; Chauhan, S. A review on mechanical and water absorption properties of polyvinyl alcohol based composites/films. *J. Mech. Behav. Mater.* **2017**, *26*, 213–222. [CrossRef]

42. Noshirvani, N.; Hong, W.; Ghanbarzadeh, B.; Fasihi, H.; Montazami, R. Study of cellulose nanocrystal doped starch-polyvinyl alcohol bionanocomposite films. *Int. J. Biol. Macromol.* **2018**, *107*, 2065–2074. [CrossRef]
43. Chiulan, I.; Frone, A.N.; Panaitescu, D.M.; Nicolae, C.A.; Trusca, R. Surface properties, thermal, and mechanical characteristics of poly(vinyl alcohol)–starch-bacterial cellulose composite films. *J. Appl. Polym. Sci.* **2018**, *135*, 45800. [CrossRef]
44. Srivastava, A.; Jain, S.; Miranda, R.; Patil, S.; Pandya, S.; Kotecha, K. Deep learning based respiratory sound analysis for detection of chronic obstructive pulmonary disease. *PeerJ Comput. Sci.* **2021**, *7*, e369. [CrossRef] [PubMed]
45. Espinosa, E.; Bascón-Villegas, I.; Rosal, A.; Pérez-Rodríguez, F.; Chinga-Carrasco, G.; Rodríguez, A. PVA/(ligno)nanocellulose biocomposite films. Effect of residual lignin content on structural, mechanical, barrier and antioxidant properties. *Int. J. Biol. Macromol.* **2019**, *141*, 197–206. [CrossRef]
46. Wang, Z.; Qiao, X.; Sun, K. Rice straw cellulose nanofibrils reinforced poly(vinyl alcohol) composite films. *Carbohydr. Polym.* **2018**, *197*, 442–450. [CrossRef] [PubMed]
47. Babu, A.G.; Saravanakumar, S.S. Mechanical and physicochemical properties of green bio-films from poly(Vinyl Alcohol)/ nano rice hull fillers. *Polym. Bull.* **2021**, *79*, 5365–5387. [CrossRef]
48. Sarwar, M.S.; Niazi, M.B.K.; Jahan, Z.; Ahmad, T.; Hussain, A. Preparation and characterization of PVA/nanocellulose/Ag nanocomposite films for antimicrobial food packaging. *Carbohydr. Polym.* **2018**, *184*, 453–464. [CrossRef] [PubMed]
49. Sultana, T.; Sultana, S.; Nur, H.P.; Khan, W. Studies on Mechanical, Thermal and Morphological Properties of Betel Nut Husk Nano Cellulose Reinforced Biodegradable Polymer Composites. *J. Compos. Sci.* **2020**, *4*, 83. [CrossRef]
50. Perumal, A.B.; Sellamuthu, P.S.; Nambiar, R.B.; Sadiku, E.R.; Phiri, G.; Jayaramudu, J. Effects of multiscale rice straw (*Oryza sativa*) as reinforcing filler in montmorillonite-polyvinyl alcohol biocomposite packaging film for enhancing the storability of postharvest mango fruit (*Mangifera indica* L.). *Appl. Clay Sci.* **2018**, *158*, 788–794. [CrossRef]
51. Khoo, R.; Ismail, H.; Chow, W. Thermal and Morphological Properties of Poly (Lactic Acid)/Nanocellulose Nanocomposites. *Procedia Chem.* **2016**, *19*, 788–794. [CrossRef]
52. Adamu, M.; Rahman, R.; Hamdan, S.; Bin Bakri, M.K.; Yusof, F.A.B.M. Impact of polyvinyl alcohol/acrylonitrile on bamboo nanocomposite and optimization of mechanical performance by response surface methodology. *Constr. Build. Mater.* **2020**, *258*, 119693. [CrossRef]
53. Zhou, P.; Luo, Y.; Lv, Z.; Sun, X.; Tian, Y.; Zhang, X. Melt-processed poly (vinyl alcohol)/corn starch/nanocellulose composites with improved mechanical properties. *Int. J. Biol. Macromol.* **2021**, *183*, 1903–1910. [CrossRef] [PubMed]
54. Syafri, E.; Yulianti, E.; Asrofi, M.; Abral, H.; Sapuan, S.M.; Ilyas, R.A.; Fudholi, A. Effect of sonication time on the thermal stability, moisture absorption, and biodegradation of water hyacinth (*Eichhornia crassipes*) nanocellulose-filled bengkuang (*Pachyrhizus erosus*) starch biocomposites. *J. Mater. Res. Technol.* **2019**, *8*, 6223–6231. [CrossRef]
55. Kohli, D.; Garg, S.; Jana, A.K. Physical, mechanical, optical and biodegradability properties of polyvinyl alcohol/cellulose nanofibrils/kaolinite clay-based hybrid composite films. *Indian Chem. Eng.* **2021**, *63*, 62–74. [CrossRef]
56. Ibrahim, M.I.J.; Sapuan, S.M.; Zainudin, E.S.; Zuhri, M.Y.M. Potential of using multiscale corn husk fiber as reinforcing filler in cornstarch-based biocomposites. *Int. J. Biol. Macromol.* **2019**, *139*, 596–604. [CrossRef] [PubMed]
57. Ong, T.; Tshai, K.; Choo, H.; Khiew, P.; Chung, S. Mechanical performance and biodegradability of polyvinyl alcohol nanocomposite films. *Mater. Werkst.* **2020**, *51*, 740–749. [CrossRef]
58. Sutka, A.; Sutka, A.; Gaidukov, S.; Timusk, M.; Gravitis, J.; Kukle, S. Enhanced stability of PVA electrospun fibers in water by adding cellulose nanocrystals. *Holzforschung* **2015**, *69*, 737–743. [CrossRef]
59. Phumma, R.; Phamonpon, W.; Rodthongkum, N.; Ummartyotin, S. Fabrication of Silver Nanoparticle Loaded into Nanocellulose Derived from Hemp and Poly(vinyl alcohol)-Based Composite as an Electrode for Electrochemical Sensors for Lactate Determination. *ACS Omega* **2024**, *9*, 10371–10379. [CrossRef]
60. Cazón, P.; Vázquez, M.; Velazquez, G. Novel composite films based on cellulose reinforced with chitosan and polyvinyl alcohol: Effect on mechanical properties and water vapour permeability. *Polym. Test.* **2018**, *69*, 536–544. [CrossRef]
61. Haghighi, H.; Gullo, M.; La China, S.; Pfeifer, F.; Siesler, H.W.; Licciardello, F.; Pulvirenti, A. Characterization of bio-nanocomposite films based on gelatin/polyvinyl alcohol blend reinforced with bacterial cellulose nanowhiskers for food packaging applications. *Food Hydrocoll.* **2021**, *113*, 106454. [CrossRef]
62. Bacha, E.G.; Demsash, H.D.; Shumi, L.D.; Debesa, B.E. Investigation on Reinforcement Effects of Nanocellulose on the Mechanical Properties, Water Absorption Capacity, Biodegradability, Optical Properties, and Thermal Stability of a Polyvinyl Alcohol Nanocomposite Film. *Adv. Polym. Technol.* **2022**, *2022*, 6947591. [CrossRef]